# Intensive Care Ultrasound

Series Editor: Gregory A. Schmidt, M.D.

# I. Physics, Equipment, and Image Quality

Rita N. Bakhru[1] and William D. Schweickert[1]

[1]Division of Pulmonary, Allergy, and Critical Care, Perelman School of Medicine, University of Pennsylvania, Philadelphia, Pennsylvania

**Keywords:** ultrasonography; echocardiography; critical care; point of care ultrasound; ultrasound physics

Ultrasound has long been accepted as a safe and accurate imaging modality for patients who are critically ill. Greater affordability and portability have made point-of-care ultrasound an available tool for the critical care physician. The initial penetration of ultrasound into the intensive care unit was driven by the success of ultrasound-guided vascular catheter insertion (1–3). Now, increasing numbers of providers are seeking broader applications to improve critical care practice. However, safe application requires a general understanding of ultrasound physics and advanced skills in image and artifact interpretation. This article is designed to introduce basic physics, equipment used, and factors that contribute to image quality.

## Wave Physics and the Generation of an Ultrasound Image

Sound is simply a series of pressure waves propagating through a medium (4, 5). Important characteristics of these waves include their frequency, amplitude, and wavelength (Figure 1). The frequency of an ultrasound wave is the number of cycles occurring in 1 second, measured in hertz (Hz). Audible sound is on the order of 2 to 20 kHz; frequencies higher than this are defined "ultrasound." Diagnostic ultrasound for medical imaging typically uses frequencies that range between 2 and 15 MHz.

The source of the ultrasound wave is the piezoelectric crystal, located in the head of the transducer (probe) (6). Image generation begins with an ultrashort electrical pulse that deforms the crystal. This deformation creates mechanical pressure waves (piezoelectric effect) that then travel out of the probe and into the adjacent medium. The crystal switches from transmission into reception mode. Ultrasound waves that have interacted with the medium reflect back and deform the crystal. This secondary deformation of the crystal generates an electric current that the machine translates into pixels, forming images on the monitor. This cycling of the piezoelectric crystal between generating pressure waves and receiving them back is repeated several thousands of times per second to create a "real-time" image.

The screen image results from information on strength, timing, and position of the returning waves. The amplitude, or strength, of the returning echo wave is translated by the machine

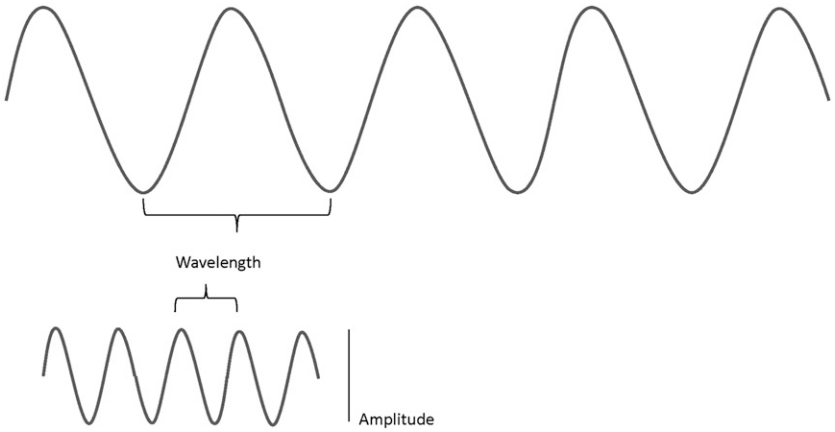


**Figure 1.** Anatomy of a wave. The top wave has a long wavelength, high amplitude, and low frequency. The bottom wave has a shorter wavelength, lower amplitude, and higher frequency.

(Received in original form June 20, 2013; accepted in final form August 13, 2013)

Supported by National Institutes of Health grant T32 HL-007891 (R.N.B.).

Correspondence and requests for reprints should be addressed to William Schweickert, M.D., 3400 Spruce Street, 5038 West Gates Building, Philadelphia, PA 19104. E-mail: william.schweickert@uphs.upenn.edu

This article has an online supplement, which is accessible from this issue's table of contents at www.atsjournals.org

This article has associated videos, which are accessible at www.atsjournals.org

Ann Am Thorac Soc Vol 10, No 5, pp 540–548, Oct 2013

DOI: 10.1513/AnnalsATS.201306-191OT
Internet address: www.atsjournals.org

into the brightness (whiteness) of an echo pixel. For example, waves leaving the transducer and reflecting fully and directly back to the transducer will maintain their high amplitude and be assigned as bright white dots on the monitor. These bright structures are termed hyperechoic. In contrast, waves that lose energy after their interaction with a structure return with low amplitude. These low-amplitude waves are translated into shades of gray—hypoechoic regions. Should the ultrasound waves encounter a structure that does not reflect any waves, no waves return back to the transducer, and the pixel on the screen appears as a black dot (anechoic).

The vertical position of the echo pixel on the screen is based on the time delay between the emission and return of the ultrasound beam. Because velocity is assumed to be constant within soft tissue, quickly returning echoes reflect superficial structures. Slowly returning echoes reflect deeper structures. Horizontal position of the echo pixel on the screen is based on the receiving piezoelectric crystal's location along the transducer. This resulting pattern of the dots' brightness and positioning in the vertical and horizontal dimensions creates the B-mode (brightness mode) image.

## Image Quality: Medium Characteristics and Wave Attenuation

Sonographic imaging is more than simple reflection of waves and is made more challenging by the complexity of human anatomy. In fact, it is the juxtaposition of structures with differing acoustic properties that makes diagnostic imaging possible. At the boundary between two tissue types, sound waves can be: (*1*) reflected directly back, like light off a mirror; (*2*) refracted, like light passing through a lens and resulting in a directional change; (*3*) scattered, sending sound waves off in all directions; or (*4*) absorbed, in which the sound wave is lost and converted to heat (Figure 2). All of these interactions reduce the intensity of the beam "attenuation" (7, 8). For practical understanding, reflection serves as the primary interaction of interest for diagnostic ultrasound and is often treated separately from attenuation.

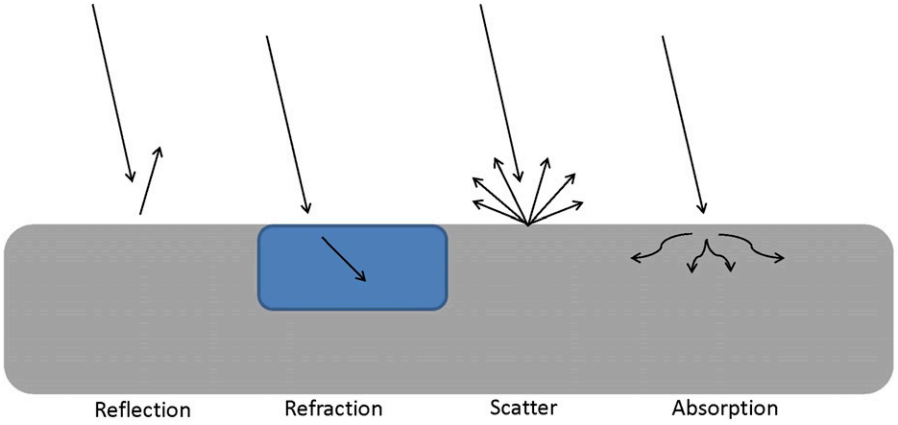


**Figure 2.** Attenuation of a wave. At the interface of two media, ultrasound waves have four potential interactions, all resulting in attenuation (reduced beam intensity).

The contrast in acoustic properties between two adjacent structures determines how much ultrasound will be reflected and how much will cross the boundary. Specifically, the variable of interest is the acoustic impedance, defined by the medium's stiffness and density. When there is a large difference in acoustic impedance, few waves cross the boundary, most will be reflected, and a strong echo will be generated. Structures with a density that is substantially different from tissue are labeled "strong reflectors." Bone has the highest acoustic


**Figure 3.** Acoustic impedance and acoustic shadowing. Image of the chest wall. Ribs (R) are present on the right and left sides of the image, recognizable by the reflection off the surface of the bone (hyperechoic line) and a posterior anechoic shadow. At the interface between the chest wall (soft tissue) and lung, the pleural surface is evident as a hyperechoic line (*). The aerated lung has a hypoechoic ("dirty") image, a second version of acoustic shadow.

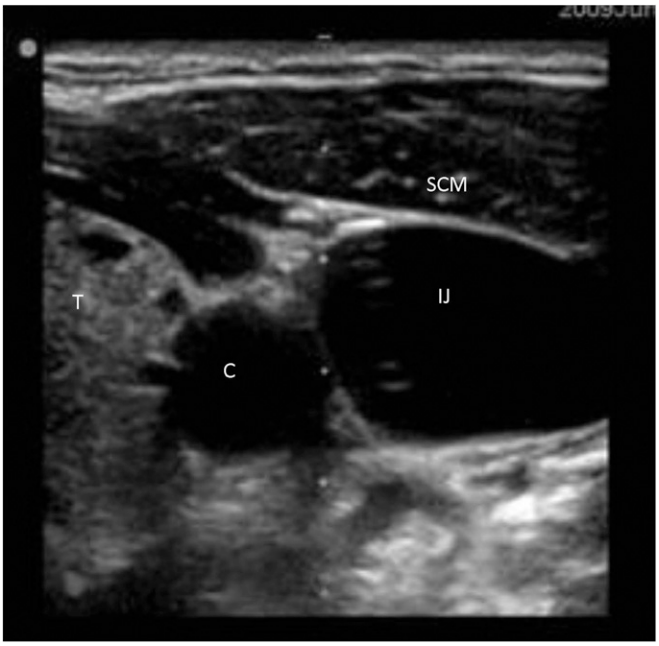


**Figure 4.** Attenuation. In this image of the neck, the sternocleidomastoid (SCM) has some attenuation, as does the thyroid (T), resulting in hyperechoic structures, whereas the fluid-filled carotid artery (C) and internal jugular (IJ) vein have little attenuation and appear anechoic.

impedance in the body; therefore, ultrasound traveling through tissue and encountering bone will be reflected, creating a hyperechoic (bright white) surface. Minimal ultrasound transmits through the bone, which is attenuated through absorption, and an anechoic (black) posterior shadow is displayed (Figure 3). A second example is the interface between soft tissue and air. Given the low density of air, the difference in acoustic impedance from tissue is similarly large. As a result, the beam reflects—appearing as a bright white line—at the soft tissue–aerated lung interface. The small air particles within the lung scatter the beam, resulting in a hypoechoic (gray) image distal to the pleura. Both of these interactions (tissue–bone, tissue–air) yield the inability to image deep structures. Both phenomena are artifacts called "acoustic shadowing."

Dense and homogenous structures have little attenuation; waves pass through them and do not lose amplitude. For example, fluid-containing structures—such as vessels, distended bladder, and cysts—have minimal wave attenuation due to the fluid's homogeneity and appear hypoechoic (dark gray) to anechoic (black) (Figure 4). In contrast, muscle and visceral organs have higher attenuation coefficients as a result of their heterogeneity and appear hyperechoic (light gray to white). The properties of the various media in human tissue and their respective ultrasound appearances are summarized in Table 1.

## Equipment

Probes (transducers) contain multiple piezoelectric crystals and vary based on the crystal arrangement, the size and shape of the imaging surface ("footprint"), and their frequency range. The three basic types of probes used in critical care ultrasound are linear, curvilinear, and phased array (Figure 5) (7, 9). Selecting the proper probe is essential; however, many diagnostic examinations benefit from the application of more than one probe.

High-frequency ultrasound is defined by the production of many waves per unit time, which engage the medium more intensely and return more waves to the probe. However, these waves lose energy more rapidly, preventing deep penetration. Therefore, high-frequency ultrasound provides high resolution of shallow structures. In contrast, lower-frequency ultrasound generates fewer waves, which travel further distances. Deeper structures can be imaged, but the fewer returning waves yield comparatively weaker resolution.

The linear array probe is designed for high-resolution imaging of superficial structures, operating at frequency ranges of 5 to 15 MHz. The linear alignment of crystals within a flat head produces sound waves in a straight line and a rectangular-shaped image on the screen. This probe is ideal for ultrasound-guided needle entry (particularly vascular access), evaluation of deep venous thrombosis, chest imaging for pleural lines (pneumothorax), and skin and soft tissue imaging for abscesses.

The curvilinear (convex) array probe is used for scanning deeper structures,

**Table 1.** Acoustic impedance and attenuation coefficients for various media and their resultant ultrasound appearance

| Medium | Acoustic Impedance ($10^6$ kg/[s×m$^2$]) | Attenuation Coefficient (dB/m at 1 MHz) | Ultrasound Appearance |
|---|---|---|---|
| Air | 0.0004 | 4,500 | Hypoechoic (high scatter) |
| Fat | 1.3 | 60 | Hypoechoic |
| Fluid | 1.5 | 6 | Very hypoechoic |
| Blood | 1.7 | 9 | Very hypoechoic |
| Liver/kidney | 1.7 | 90 | Echogenic |
| Muscle | 1.7 | 350 | Echogenic |
| Bone | 7.8 | 870 | Hyperechoic surface with anechoic posterior shadow |

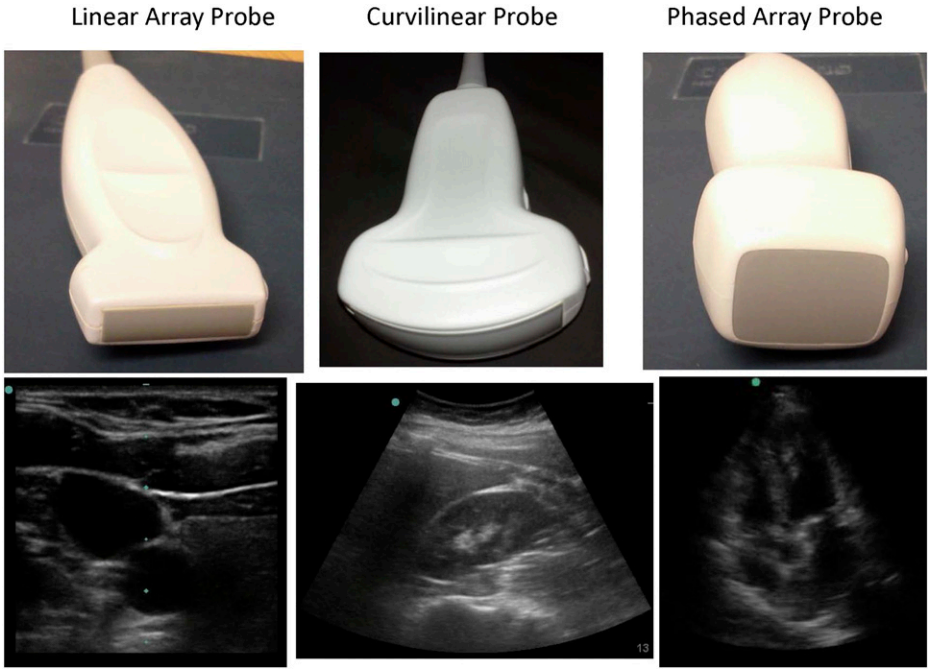


**Figure 5.** Ultrasound probes. Examples of the three types of probes used in critical care ultrasonography, with a corresponding example of an image from each type of probe.

using lower frequencies ranging between 1 and 8 MHz. The crystal alignment along a curved surface generates a beam that fans outward. The result is a field of view wider than the probe's footprint, with a sector-shaped image on the screen. These probes are most often used in abdominal and pelvic diagnostic applications.

The phased array probe is a lower-frequency probe (ranging 1–10 MHz) that is novel in its sequential pulsing of the tightly grouped crystals. By precisely controlling delays between pulses, beams of various angles and focal distances can be produced for inspection of complex structures. The smaller footprint allows for image acquisition between the ribs, and the slightly convex surface produces a fanning beam with a sector-shaped image. This probe is used for echocardiography and thoracic imaging but can be applied to abdominal and pelvic imaging as well.

All ultrasound probes have a raised marker or indentation (Figure 6) that correlates with the side of the screen marked with an identifier (usually a dot or the manufacturer's logo). Structures close to the probe marker will appear on the side of the image with the screen marker, helping to orient the viewer and guide probe manipulations. For example, when imaging the right internal jugular vein when working from the head of the bed, the probe marker is toward the patient's left when the screen marker is on the left. Accordingly, medial structures are

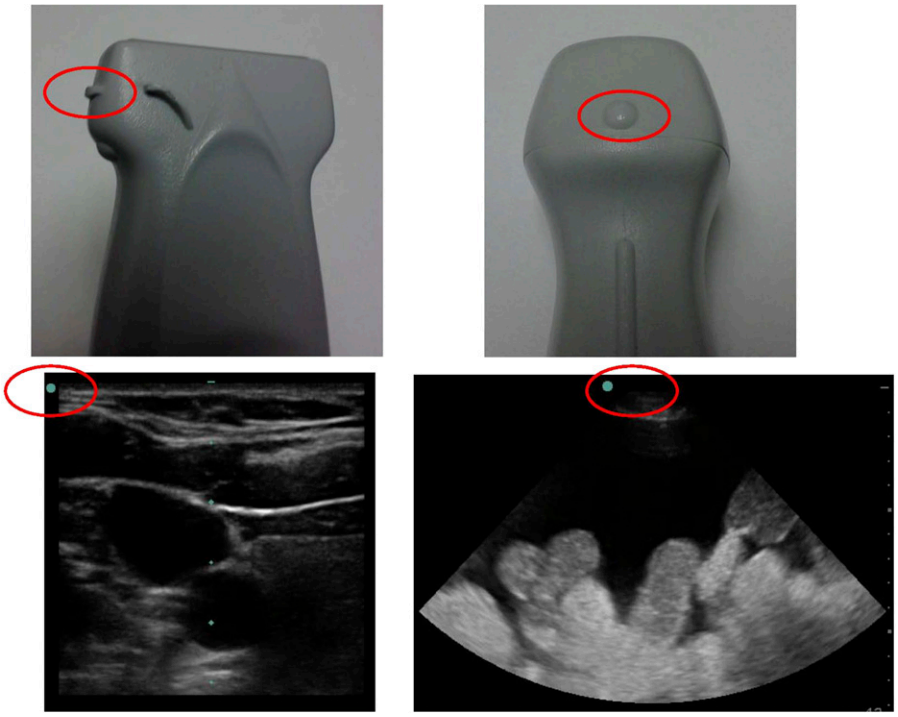

**Figure 6.** Probe markers. Each probe has a marker that correlates with the dot (or manufacturer's logo) on the screen.

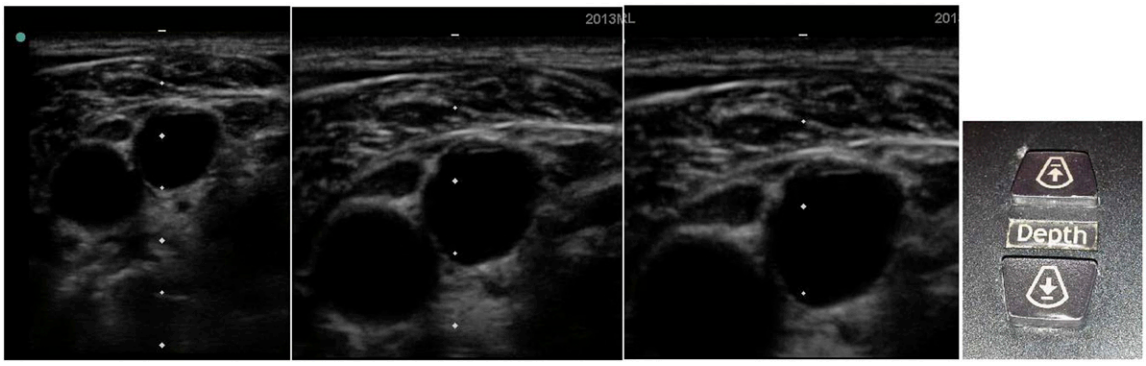


**Figure 7.** Depth. As the depth is decreased from left to right, the internal jugular and the carotid artery come closer into view. The depth button on the console (*right panel*) is used for adjustments.

positioned on the left side of the screen (e.g., thyroid), and lateral structures (e.g., internal jugular vein) are on the right side of the screen. Diagnostic imaging by radiologists and emergency medicine clinicians has positioned the screen marker on the left by convention. In contrast, the standard acquisition of images in echocardiography examinations places the marker in the upper right corner of the screen. The user can adjust the screen marker position to the upper left or right side; either orientation may be used. We advocate for the novice sonographer to begin scanning along the standard axes (transverse, longitudinal, coronal) with a uniform probe marker orientation. As sonography skills mature, oblique planes become interpretable.

## Image Manipulation

To maximize the diagnostic quality of ultrasound images, depth and gain may need to be modified by the operator. Depth, manipulated on the console, is a measure of how far ultrasound waves will penetrate and determines the number of centimeters of tissue displayed on the monitor (Figure 7). The operator should alter the depth on the screen to position the structure of interest in the mid to lower third of the screen. This is the default site of the focal zone, defined as the region where the ultrasound beam is narrowest. As a result, lateral resolution—the ability to discriminate between two side-by-side structures—is optimal. Should the structure of interest be superficial and located in the proximal screen, adjusting the focal zone to this territory may be necessary (as machine function permits).

Gain adjusts the brightness of the entire image (Figure 8) but does not affect resolution or pixels per image. Gain manipulation capabilities are machine dependent. Some machines adjust overall screen gain, others partition the screen into proximal and distal halves, and only select point-of-care machines adjust gain at a variety of depths (time gain compensation).

Image resolution is determined by the frequency and duration of the transmitted pulse. Axial resolution refers to the ability to resolve objects within the imaging plane at different depths parallel to the direction of the pulse. Axial resolution is best with higher-frequency probes and their short pulses. As described above, lateral resolution refers to the ability to resolve objects in the imaging plane that are located side by side.

## Ultrasound Artifacts

In pursuit of an accurate representation of anatomy, the ultrasound machine makes a number of assumptions about sound propagation in tissue. However, tissue heterogeneity gives rise to visible image artifacts. These artifacts assume different forms in the displayed image, including perceived objects that are not actually present, structures that should be represented but are missing, and structures whose locations are incorrectly registered (4). Most artifacts interfere with image interpretation; however, some contain diagnostically useful clues. Their recognition and

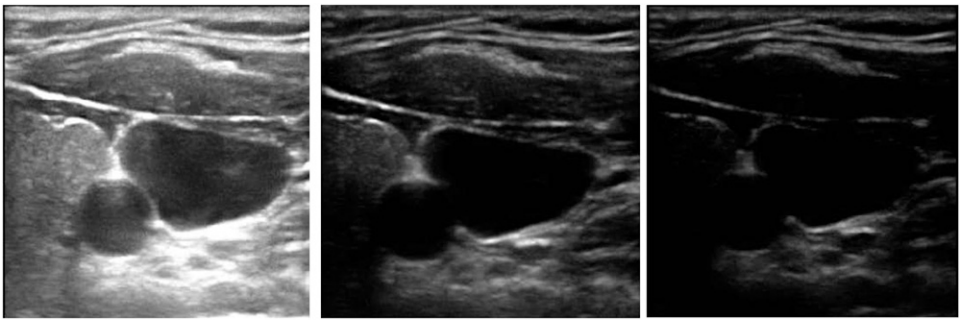

**Figure 8.** Gain. In the center is an image of the neck (with carotid artery and internal jugular vein at the center), with a normally adjusted gain. On the left, the gain has been increased, resulting in a brighter (more hyperechoic) overall image. On the far right, the gain has been decreased, resulting in an overall darker image.


**Figure 9.** Acoustic shadowing. On the left there is a vessel (V) with a catheter (*) in it. Posterior to the catheter is an acoustic shadow (A).

interpretation is an essential skill of the proficient sonographer. Potential clues to identification of an artifact include: (*1*) artifacts radiate from the top of the screen (or the head of the probe), (*2*) artifacts move with probe movements, and (*3*) artifacts are linear and regular in contrast to normal anatomy (10).

Acoustic shadowing, described above, is the most commonly encountered artifact. It can serve as a diagnostic hindrance by obscuring deep structures (e.g., shadows deep to rib). In some cases, it can aid in the recognition of a solid structure; examples include cholelithiasis or the intravascular position of a catheter (Figure 9) (11, 12). Similarly helpful is the shadowing behind an air interface (scattered beam at tissue/gas interfaces); it can serve as an affirmation of lung aeration.

Conversely, posterior acoustic enhancement (Figure 10) occurs when there is an artifactual brightness deep to an anechoic structure, often a cyst or blood vessel (13). Waves passing through the fluid-containing structure are less attenuated than waves passing through adjacent tissue. The imaging result is a relative increase in echogenicity (due

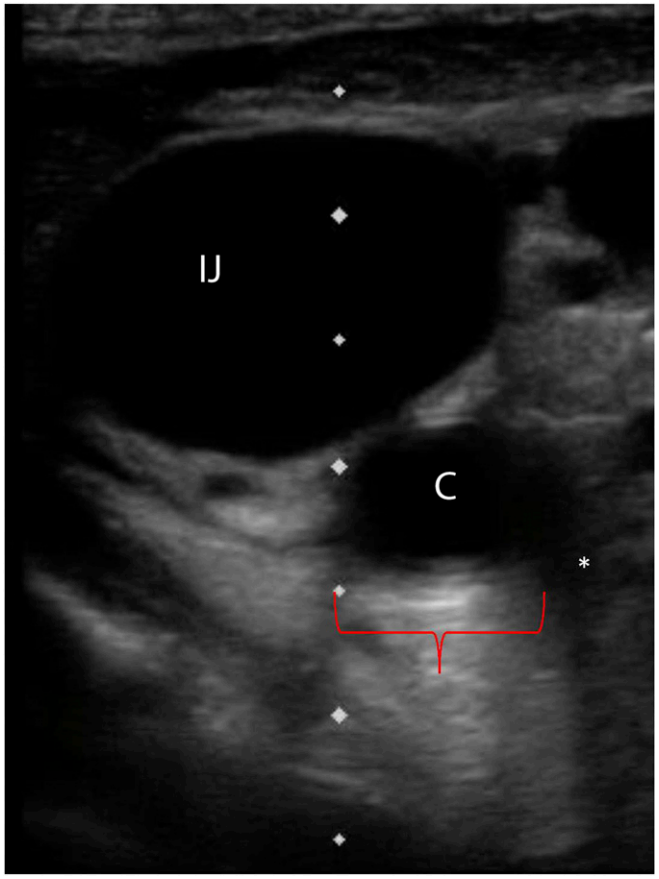


**Figure 10.** Posterior acoustic enhancement and refraction artifact. The internal jugular vein (IJ) and the carotid artery (C) are shown. Posterior to the carotid (*red bracket*) is an area of increased echogenicity due to posterior acoustic enhancement. At the medial edge posterior to the carotid, refraction artifact (*) is seen.

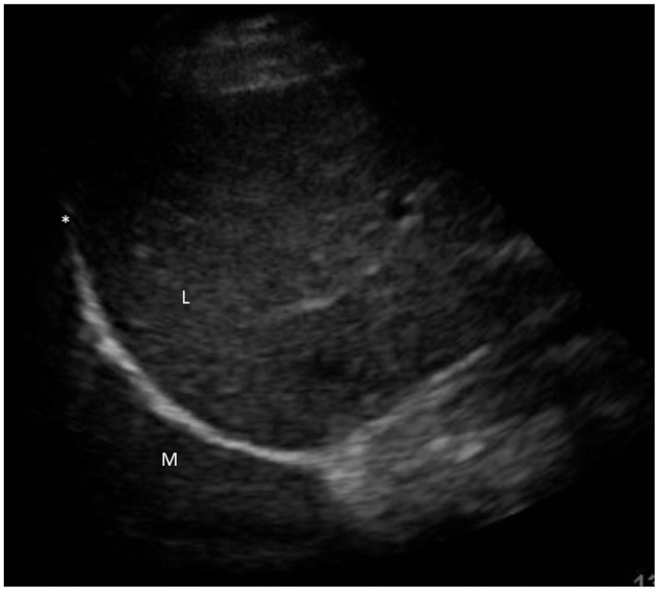


**Figure 11.** Mirror image artifact. The liver (L) is seen with the diaphragm adjacent. Deep to the highly echogenic diaphragm (*) is a mirror image of the liver (M).

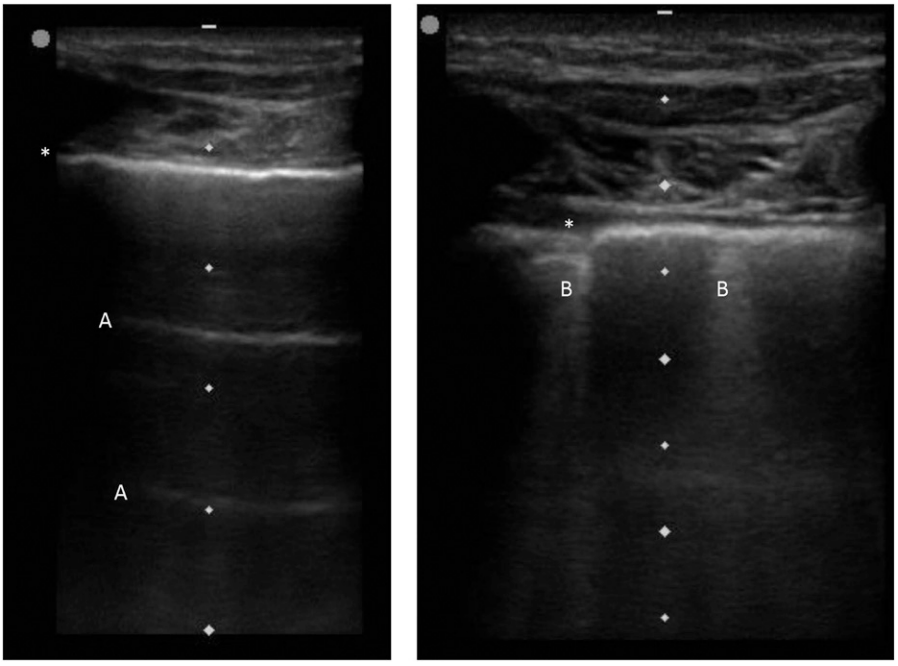


**Figure 12.** Reverberation artifact. On the left, the pleural surface is marked (*). Deep to it are A-lines (A), artifacts from the soft tissue–air interface. On the right, the pleural surface is again marked (*). From the pleural surface, B-lines (B), artifacts from interstitial edema, radiate distally.

to more energy returning to the transducer) in tissues deep to the fluid-containing structure. Posterior acoustic enhancement can be used to distinguish cysts and fluid collections from solid masses.

Mirror images (Figure 11) occur when sound waves undergo multiple reflections and create an artifact (14). Generally, sound waves that encounter a strong reflector will generate accurate images of a proximal object and its adjacent reflector. However, the reflector causes some waves to be reflected backward, resulting in a longer travel time and miscalculation of depth by the ultrasound machine. This results in the image proximal to the reflector being duplicated on the other side of the strong reflector. The classic example of a mirror image is an artifactual appearance of the liver cephalad to the diaphragm. The mirror image will disappear with changes in position of the transducer, whereas the real image is visible in multiple planes.

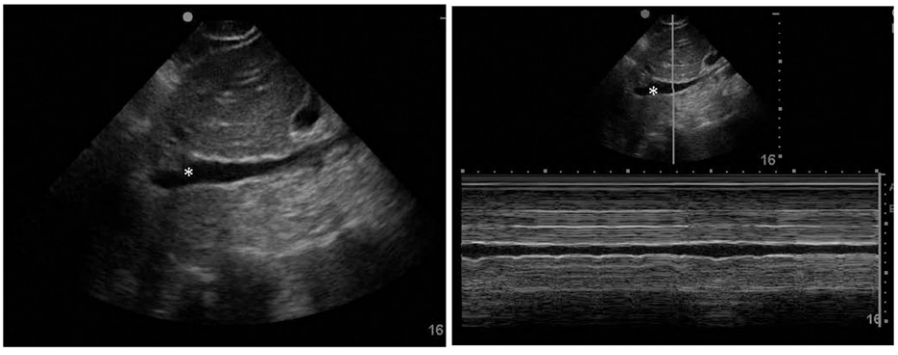


**Figure 13.** M-mode. At left is a longitudinal image of the inferior vena cava (IVC, *). At right is an M-mode image of the IVC. The display of IVC caliber versus time allows measurement of IVC collapsibility with respiration.

Reverberation artifact occurs when sound waves bounce back and forth between two highly reflective structures (Figure 12). For example, scans of normally aerated lung may depict A-lines: recurrent hyperechoic horizontal arcs, parallel to the pleural line and arising below it, each appearing at an identical interval (distance) to the one between skin and pleural line (15). These lines are artifacts caused by repeated reflections between the skin/transducer interface and the pleura. The delayed return of multiply reflected waves is interpreted and plotted as a deeper structure by the machine. The absence of A-lines indicates that there has been a fundamental change in the attenuation coefficient of the lung, such as pulmonary edema or consolidation. A second example, also from the lungs, is the appearance of B-lines, a comet tail artifact (16). These vertical hyperechoic lines extend from the pleural line to the lower edge of the image and move with respiratory variation (Video 1). This artifact is caused by sound waves trapped in fluid-filled intralobular or interlobular septa touching the visceral pleural surface (17, 18). Other scenarios with reverberation artifact, sometimes referred to as ring-down artifact, are generated by strong reflectors that include gas collections in the body (e.g., free peritoneal air) and metallic foreign bodies (e.g., needle insertion, staples, shrapnel) (19).

A final common artifact is refraction artifact, or edge shadowing (Figure 10). This occurs when a sound wave obliquely encounters the edge of the curved surface resulting in beam divergence. This energy loss leads to the formation of a shadow, most commonly along the edge of a cyst or vessel in transverse orientation.

## Other Modes

M-mode (motion mode) is used to display and measure the movement of structures over time. This mode is commonly used to assess respiratory changes in inferior vena cava diameter, cardiac valve excursion, and dynamic movement of the lung for evaluation of pneumothorax (10, 20). To accomplish this, the structure of interest is initially localized in B-mode (Video 2). A

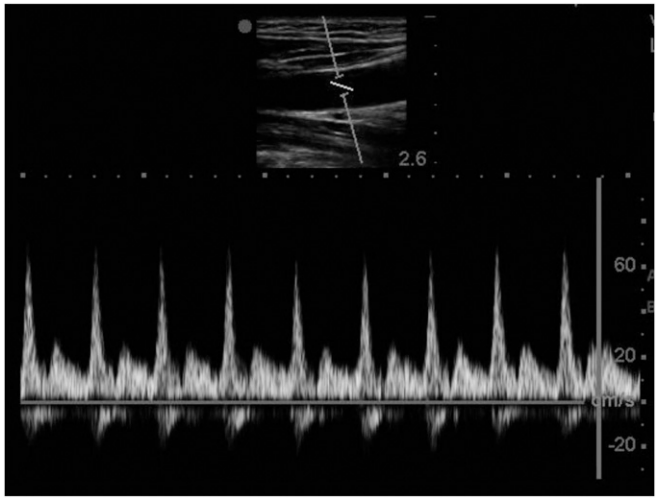


**Figure 14.** Spectral ultrasound. The vessel is imaged in B-mode with a gate positioned across the vessel (*top*). The spectral Doppler displays flow (cm/sec) versus time. This picture demonstrates the arterial waveform of the carotid artery.

vertical cursor is positioned to acquire structural changes along that cursor line. Once engaged, M-mode then displays the one-dimensional scan line on the vertical axis and time on the horizontal axis (Figure 13).

Doppler ultrasound detects a change in frequency from the sent to the returning sound wave as a result of the sound waves interacting with moving particles, such as red blood cells. Red cells flowing toward the transducer reflect a higher frequency; those flowing away from the transducer reflect a lower frequency. The amount of frequency shift correlates with the velocity and direction of particle motion. In sum, Doppler mode examines the characteristics of direction and speed of blood flow (and tissue motion) and presents them in audible, color, or spectral display.

In color Doppler, blood flow directionality and velocity are represented by shades of red and blue. An imaging gate is applied across the structure, and areas of flow within the region are depicted in color (Video 3). A legend on the screen demonstrates the directional color assignment (e.g., blue demonstrates blood flow toward the transducer and red depicts flow away). Velocity is represented by the color bar; the color most distal to the central black color represents the fastest movement. Power Doppler, a subset of color Doppler, is more sensitive in detecting slow-flow movement but does not measure speed or direction of flow (Video 4). This mode displays regions with flow in color and can be helpful to screen subcutaneous tissue for vascular structures in a planned needle pathway (e.g., paracentesis).

For spectral Doppler (Figure 14), the machine represents the movement of blood via (*1*) an audible flow sound, and (*2*) a graph depicting flow velocities in relation to time. Continuous-wave spectral Doppler measures all velocities along a path and excels at resolving velocity (but not position). This is used most commonly to estimate pulmonary artery pressures by measuring tricuspid regurgitant velocities. In contrast, pulsed-wave spectral Doppler sacrifices sensitivity to the highest velocities in exchange for spatial resolution. This mode is ideal for measuring lower velocities at chosen anatomic locations, as when estimating stroke volume from the left ventricular outflow tract. ■

**Author disclosures** are available with the text of this article at www.atsjournals.org.

## References

1 Randolph AG, Cook DJ, Gonzales CA, Pribble CG. Ultrasound guidance for placement of central venous catheters: a meta-analysis of the literature. *Crit Care Med* 1996;24: 2053–2058.
2 Hind D, Calvert N, McWilliams R, Davidson A, Paisley S, Beverley C, Thomas S. Ultrasonic locating devices for central venous cannulation: meta-analysis. *BMJ* 2003;327:361.
3 Maecken T, Grau T. Ultrasound imaging in vascular access. *Crit Care Med* 2007; 35(5 Suppl):S178–S185.
4 Hedrick WR, Hykes DL, Starchman DE. Ultrasound physics and instrumentation. 4th ed. St. Louis, MO: Elsevier Mosby; 2005.
5 Hoskins P. Diagnostic ultrasound: physics and equipment. London; San Francisco: Greenwich Medical Media: Distributed in the USA by Jamco Distribution; 2003.
6 Hangiandreou NJ. AAPM/RSNA physics tutorial for residents. Topics in US: B-mode US: basic concepts and new technology. *Radiographics* 2003;23:1019–1033.
7 Lawrence JP. Physics and instrumentation of ultrasound. *Crit Care Med* 2007; 35:S314–S322.
8 Allan PLP, Baxter GM, Weston MJ. Clinical ultrasound. 3rd ed. Edinburgh: Churchill Livingstone; 2011.
9 Aldrich JE. Basic physics of ultrasound imaging. *Crit Care Med* 2007; 35(5 Suppl):S131–S137.
10 Lichtenstein D. Whole body ultrasonography in the critically ill. Heidelberg: Springer; 2010.
11 Maury E, Guglielminotti J, Alzieu M, Guidet B, Offenstadt G. Ultrasonic examination: an alternative to chest radiography after central venous catheter insertion? *Am J Respir Crit Care Med* 2001;164: 403–405.
12 Schweickert WD, Herlitz J, Pohlman AS, Gehlbach BK, Hall JB, Kress JP. A randomized, controlled trial evaluating postinsertion neck ultrasound in peripherally inserted central catheter procedures. *Crit Care Med* 2009;37:1217–1221.
13 Feldman MK, Katyal S, Blackwood MS. US artifacts. *Radiographics* 2009;29:1179–1189.
14 Noble VE, Nelson B. Manual of emergency and critical care ultrasound. 2nd ed. Cambridge: Cambridge University Press; 2011.
15 Lichtenstein D, Goldstein I, Mourgeon E, Cluzel P, Grenier P, Rouby JJ. Comparative diagnostic performances of auscultation, chest radiography, and lung ultrasonography in acute respiratory distress syndrome. *Anesthesiology* 2004;100:9–15.
16 Lichtenstein D, Mézière G, Biderman P, Gepner A, Barré O. The comet-tail artifact. An ultrasound sign of alveolar-interstitial syndrome. *Am J Respir Crit Care Med* 1997;156: 1640–1646.

17 Agricola E, Bove T, Oppizzi M, Marino G, Zangrillo A, Margonato A, Picano E. "Ultrasound comet-tail images": a marker of pulmonary edema: a comparative study with wedge pressure and extravascular lung water. *Chest* 2005;127: 1690–1695.
18 Jambrik Z, Monti S, Coppola V, Agricola E, Mottola G, Miniati M, Picano E. Usefulness of ultrasound lung comets as a nonradiologic sign of extravascular lung water. *Am J Cardiol* 2004;93:1265–1270.
19 Avruch L, Cooperberg PL. The ring-down artifact. *J Ultrasound Med* 1985;4:21–28.
20 Breitkreutz R, Walcher F, Seeger FH. Focused echocardiographic evaluation in resuscitation management: concept of an advanced life support-conformed algorithm. *Crit Care Med* 2007;35:S150–S161.